



## NUMERICAL SIMULATIONS FOR DETERMINING THE THERMAL RESPONSE OF WALL SYSTEMS WITH MEDIUM DENSITY POLYURETHANE SPRAY FOAMS

Tariku\* F, Maref W, Swinton M.C. and Elmahdy A.H.  
National Research Council, Canada (NRCC)  
Institute for Research in Construction (IRC)  
Ottawa, Canada  
www.irc.nrc-cnrc.gc.ca  
Contact: Wahid.maref@nrc-cnrc.gc.ca

### ABSTRACT

Using Polyurethane Spray Foams (SPFs) as insulation in buildings provide durable and efficient thermal barriers. The industry is encouraging the SPF as an effective air barrier system in addition to its thermal insulation characteristics. In an effort to address these issues, a consortium of SPF manufacturers and contractors, jointly with the National Research Council of Canada's Institute for Research in Construction, (NRC-IRC) conducted an extensive research project to assess the thermal and air leakage characteristics of SPF walls. Walls with glass fibre insulation and polyethylene air barrier were also considered as references. A number of walls with different types of SPFs and glass fibre were built and tested. Material characterization was also conducted to measure the thermal conductivities of a number of SPFs. Additionally, the thermal resistances (R-values) of these walls were measured using Guarded Hot Box (GHB) at two temperature differences across the walls (40 & 55°C) and zero air leakage (i.e. pressure differences across the wall was 0). In order to investigate the effect of the air leakage on the R-values, however, air leakage tests were conducted for these walls at a wide range of pressure differences across the walls (25 Pa - 170 Pa).

The objective of this paper is to conduct 2D numerical simulations to determine the R-values with and without air leakage. These simulations were conducted using the advanced hygrothermal model that was developed by the NRC-IRC. The results showed that the model was successful in predicting the R-values with reasonably good agreements with the measured R-values using the GHB. After gaining confidence in predicting the R-values at no air leakage, a parametric study was conducted to predict the apparent R-values at two leakage rates that correspond to two pressure differences of 75 Pa and 150 Pa for each wall.

### INTRODUCTION

Spray Polyurethane Foam insulation (SPF) has been gaining<sup>1</sup> considerable attention in North America for a number of reasons, including: the claimed better thermal performance of foamed walls relative to conventional poly-wrapped batt insulated walls; better air leakage performance, and the introduction of environmentally friendly blowing agents to reduce greenhouse gas emission. A few years ago, the North American SPF industry joined forces to develop a replacement of the commonly used chlorofluorocarbon blowing agent. The introduction of the second generation of blowing agents (namely hydrochlorofluorocarbon, HCFC) was seen as a positive step in the processing of SPF. Other agents were also developed and their performance was assessed and reported by Bomberg & al. (1989) and Kumar & al. (1990). In recent years, the focus of building code and regulatory officials, professionals and researchers has shifted towards the performance of the entire wall system. The emphasis is on the contribution of SPF and other insulated walls to the control of heat, moisture and air through the system. Therefore, it is not sufficient to characterize the wall by its R-value alone, as was the case in the past.

This paper is one in a series to present information generated from a research project conducted jointly by the National Research Council Institute for Research in Construction (NRC-IRC) and the polyurethane industry (contractors, and material suppliers) to assess the overall performance of insulated walls. In an earlier paper written by Elmahdy & al. (2009), the authors presented a brief outline of the project objectives and a limited set of results of two walls that were available at that time. The test results of six walls were published later by Maref & al. (2009). These walls included two glass fibre poly-sealed walls (reference walls) as well as four walls of medium density foam (closed cell foam) insulation.

---

\*Formerly at NRC-IRC during this research project and now at British Columbia Institute of Technology (BCIT) Burnaby, BC, Canada.

## OBJECTIVES

The main project objective is to develop experimental and analytical procedures to determine the energy rating of SPF walls (WER). In addition, the foam producers and applicators desired to demonstrate that the use of polyurethane spray foam (when applied with certified foamers to ensure the intended thickness, and at the right temperature and relative humidity ) could also provide an air barrier system that could meet the Canadian Construction Material Centre (CCMC) guide 07272 (Di Lenardo, 1995). Therefore, the project is aimed at demonstrating these features, both analytically and experimentally to see as well the effect of air leakage on the overall thermal performance of the wall system insulated with SPF and with glass fibre batts and polyethylene-based air barrier. This project also aims to develop a calculation tool to help practitioners to design their insulated walls taking into account the effect of the air leakage to assess their thermal performance; for example: to calculate the apparent R-value at 75 Pa for a given wall knowing the R-value at no air leakage. The objective of this paper is to conduct 2D numerical simulations to determine the R-values with and without air leakage. These simulations were conducted using the advanced hygrothermal model that was developed by the NRC-IRC.

## DESCRIPTION OF HYGROTHERMAL MODEL

A detailed description of the advanced hygrothermal model hygIRC was previously published by Karagiozis (1993, 1997), Salonvaara and Karagiozis (1994) and Hens (1996). Here, a brief description of the mathematical model is presented. The model solves, simultaneously, the three interdependent transport phenomena of heat, air and moisture in a building component. The mathematical model is based on building physics and comprises a set of partial differential equations that govern the individual flows. The corresponding governing equations are as follow:

Moisture balance:

$$\frac{\partial w}{\partial t} + \nabla \cdot (\vec{u} \rho_v + K \rho_w \vec{g}) = \nabla \cdot (D_w \nabla w + \delta_p \nabla p_v) + \dot{m}_s \quad (1)$$

Heat balance:

$$c \rho_o \frac{\partial T}{\partial t} + \nabla \cdot (\vec{u} \rho_a c_{p,a} T) = \nabla \cdot (\lambda \nabla T) + L_v [\nabla \cdot (\delta_p \nabla p_v)] - L_{ice} \left( w \frac{\partial f_l}{\partial t} \right) + \dot{Q}_s \quad (2)$$

Air mass balance:

$$\nabla \cdot (\rho_a \vec{u}) = 0 \quad (3)$$

Momentum balance (Darcy equation):

$$\vec{u} = -\frac{k_a}{\eta} \nabla P \quad (4)$$

$$-\nabla \cdot \left( \rho_a \frac{k_a}{\eta} \nabla P \right) = 0 \quad (5)$$

where:  $w$ =moisture content (kg/m<sup>3</sup>);  $\vec{u}$ =air velocity (m/s);  $\rho_v$ =water vapour density (kg/m<sup>3</sup>);  $K$ =liquid water permeability (s);  $\rho_w$ =density of water (kg/m<sup>3</sup>);  $\vec{g}$ =acceleration due to gravity (m/s<sup>2</sup>);  $D_w$ =moisture diffusivity (m<sup>2</sup>/s);  $\delta_p$ =vapour permeability (s);  $p_v$ =vapour pressure (Pa);  $\dot{m}_s$ =moisture source (kg/m<sup>3</sup>);  $c$ =effective heat capacity (J/kg.K);  $\rho_o$ =dry density of the material (kg/m<sup>3</sup>);  $T$ =temperature (°C);  $\rho_a$ =density of air (kg/m<sup>3</sup>);  $c_{p,a}$ =specific capacity of air (J/kg.K);  $\lambda$ =effective thermal conductivity (W/m.K);  $L_v$ =latent heat of evaporation/condensation (J/kg);  $L_{ice}$ =latent heat of freezing/melting (J/kg);  $f_l$ =fraction of water frozen (-);  $\dot{Q}_s$ =heat source (W/s.m<sup>3</sup>);  $k_a$ =air permeability (m<sup>2</sup>); and  $\eta$ =dynamic viscosity (kg/ms).

The driving potentials of moisture transport, Equation(1), are vapour pressure and moisture content. The advanced model includes two important moisture transport mechanisms, in addition to diffusion process: water vapour transport by convection and liquid water transport by gravity as expressed by the second and third terms of the left hand side of the equation, respectively. The model also has the capability of handling volumetric moisture sources or sinks as represented by the last term in the right hand side of the equation. Temperature is the driving potential for the heat balance equation, Equation (2). The transfer of heat by convection and diffusion are represented by the second (l.h.s) and first (r.h.s) terms of the equations, respectively. The heat source or sink associated with phase changes are represented by the second (evaporation/condensation) and third (freeze-thaw) terms of the right hand side of the equation. Any other internal heat source or sink is given by the last term of the right hand side of the equation. The mass balance equation for incompressible fluid is given by Equation (3). The Darcy equation, Equation (4), is a reduced form of the Navier-Stokes momentum equation for flow in a porous medium. In a building physics application, the air is considered as incompressible due

to very low airflow speeds, and low pressure and temperature changes. Combining the mass balance, (Equation (3)) and momentum balance (Equation (4)) equations gives Equation (5). The model was extensively benchmarked in a number of client and strategic projects (Maref et al. 2002a, 2002b; Tariku and Kumaran, 2006; Maref and Tariku, 2007; Tariku et al., 2007).

In this paper, hygIRC-2D is used for the simulation of combined conduction-convection heat transfer in the six wall assemblies described above. Here, the model's application, however, is limited to steady-state heat transfer and airflow aspects. In this case, where the effect of moisture on heat transfer is neglected, the hygIRC-2D governing equation for heat transfer Equation (2) is reduced to Equation (6). As can be seen in this equation, the model accounts for heat transfer by conduction (r.h.s first term) as well as by convection (l.h.s second term). The airflow velocity ( $\vec{u}$ ) that is required in this equation is computed from the pressure field in the computational domain, which is computed using Equation (5).

$$c\rho_o \frac{\partial T}{\partial t} + \nabla \cdot (\vec{u}\rho_a c_{p,a}T) = \nabla \cdot (\lambda \nabla T) \quad (6)$$

## CONDUCTION-CONVECTION HEAT TRANSFER ANALYSIS

### Methodology

Heat transfer across a wall assembly involves multi-dimensional heat exchanges within the wall structure. The multi-dimensional heat flows are due to the thermal bridges that are created by the wood frames and air movement due to natural and forced convections. In thermal bridge areas there is a temperature gradient that promotes heat transfer in the lateral direction in addition to the primary heat flow direction. Figure 1 shows the temperature profile around an SPF wall stud in a plan view. In this case, the exterior and interior surface of the wall assembly are exposed to  $-5^\circ\text{C}$  and  $20^\circ\text{C}$ , respectively. As shown in Figure 2, the temperature difference across the same wall assembly creates air movement in the third dimension: the vertical direction. This air circulation (convection loop) facilitates heat transfer by convection and mixing. To capture these multi-dimensional effects in the simulation, the three dimensional wall system is divided into three zones as shown in Figure 3, in green, yellow and blue. The regions represent the wall sections with minimum and maximum stud effects, and frame junction regions, respectively. The heat flow through a region where the stud and top (or bottom) plate join (frame junction region) is assumed to be one-

dimensional heat transfer and is calculated by taking into account the thermal resistances of the sheathing board, top (or bottom) plate and interior layer (gypsum board).

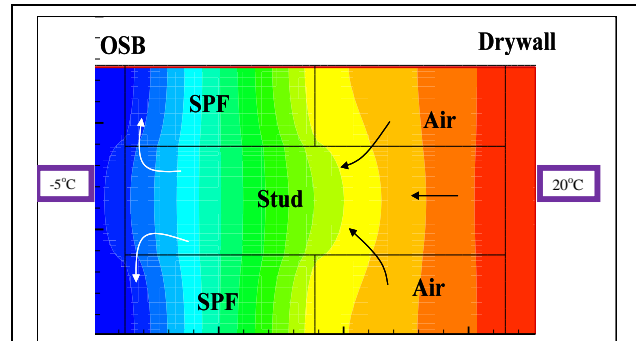


Figure 1. Temperature contour plot around SPF insulated wall stud (Plan view)

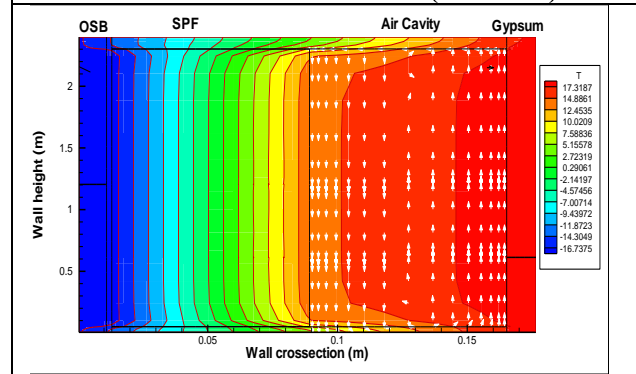


Figure 2. Convection loop in the air cavity of SPF insulated wall assembly

The region with maximum stud influence (yellow region) is composed of the stud and 1.5" insulation on each side. The airflow and its effect in the thermal analysis are captured by a two-dimensional analysis of the region with minimum stud effect (green region). The vertical and horizontal cross-sections of the respective zones, Section A-A and Section B-B (Figure 4), define the hygIRC-2D computational domain of the respective zones. The basic assumptions that are made in the two-dimensional heat transfer simulations of these two regions are: there is no lateral heat transfer and vertical heat transfer in the representative sections A-A and B-B, respectively. Finally, the overall RSI value of a wall assembly is computed based on the two-dimensional simulation results of the two regions using Equation (7).

$$RSI = A \frac{DT}{(q_v A_v + q_h A_h + q_j A_j)} - R_s \quad (7)$$

Where:  $A_v$ : vertical cross-sectional area,  
 $A_h$ : Horizontal cross-sectional area,  
 $A_j$ : Stud and horizontal plate junction area  
 $A$ : Total wall area,  
 $DT$ : Air temperature difference,  
 $q_v$ : Heat flow through the vertical cross-section,  
 $q_h$ : Heat flow through the horizontal cross-section,  
 $q_j$ : Heat flow through the junction area,  
 $R_s$ : Surface thermal resistance, given as

$$R_s = \left( \frac{1}{h_i} + \frac{1}{h_e} \right),$$

where  $h_i$  and  $h_e$  are the internal and external heat transfer coefficients, respectively.

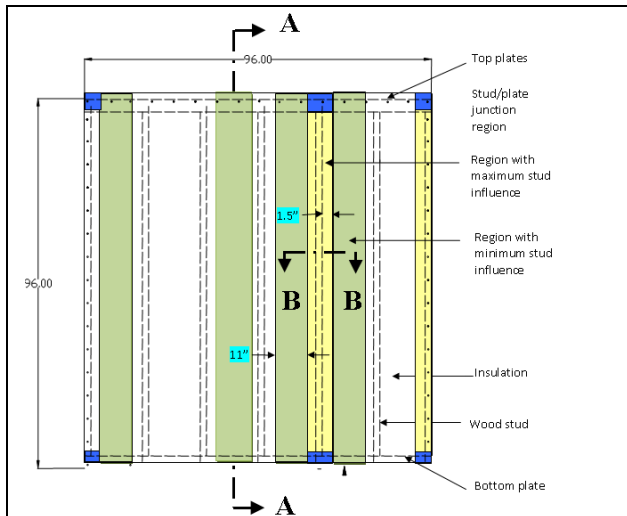


**Figure 3. Front view of a typical glass fiber insulated wall assembly**

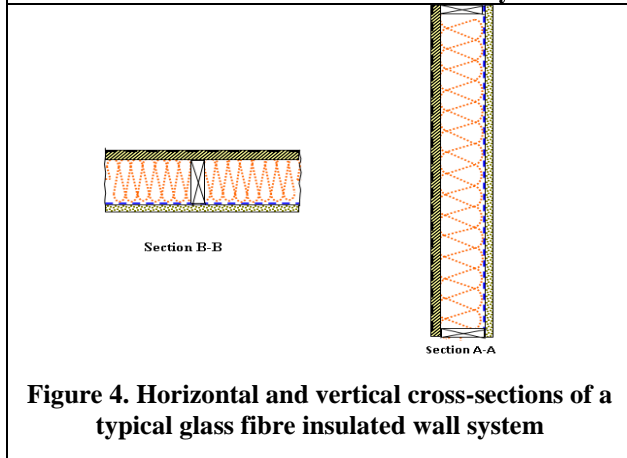


**Figure 4. Horizontal and vertical cross-sections of a typical glass fibre insulated wall system**

In simulation cases where forced convection (air leakage) through the wall assembly is considered, the

apparent RSI (RSI\*) is calculated based on Equation (8) to take account the conduction and convection heat losses.

$$RSI^* = A \frac{DT}{(q_v A_v + q_h A_h + q_j A_j + Q_{air})} - R_s \quad (8)$$

Where  $Q_{air}$  is the heat loss due to air leakage.

## SIMULATION PARAMETERS

### Simulation input parameters

The two basic parameters that are required to conduct the combined conduction-convection thermal analysis of the six 2” by 6” wood-frame wall assemblies using the computer model described above are: material properties and air leakage characteristics of the wall systems. In Table 1, the thickness and thermal conductivities of the materials that make up the wall assemblies are presented. These thermal conductivity values are taken from Kumaran et al. (2002) except that of SPF, which is measured within the project and reported in Elmahdy et al. (2009). Table 2 summarizes the air leakage characteristics of the six walls at 75 and 150 Pa pressure differences. The air leakage tests were conducted in the laboratory according to ASTM Standard 232.

**Table 1. Physical and thermal conductivity of the materials in the wall assembly**

| Wall layer                 | Thickness (mm) | Thermal conductivity W/(m.K) |
|----------------------------|----------------|------------------------------|
| Spruce                     | 152            | 0.090                        |
| OSB                        | 13             | 0.090                        |
| Glass fibre                | 152            | 0.039                        |
| Gypsum board               | 12             | 0.159                        |
| Expanded polystyrene       | 102            | 0.029                        |
| Spray foam (WER 2, WER 3A) | 102            | 0.020                        |
| Spray foam (WER 3B)        | 102            | 0.019                        |
| Spray foam (WER 4)         | 102            | 0.018                        |

**Table 2. Air leakage characteristics of the six walls at 75 and 150Pa pressure difference**

| Wall ID | Air leakage rate (L/s.m <sup>2</sup> ) |                             |
|---------|--|-----------------------------|
|         | @75 Pa pressure difference             | @150 Pa pressure difference |
| WER 1   | 0.369                                  | 0.657                       |
| WER 2   | 0.013                                  | 0.026                       |
| WER 3A  | 0.046                                  | 0.061                       |
| WER 3B  | 0.034                                  | 0.049                       |
| WER 4   | 0.059                                  | 0.117                       |
| WER 5   | 0.620                                  | 1.123                       |

## Airflow path assumption

As mentioned earlier, the effect of air leakage on the thermal performance of a wall assembly is a focus of the study. The principal driving pressure for air leakage can be due to wind pressure, indoor and outdoor temperature differences (stack-effect) or a combination of the two. Although the air leakage characteristics of the walls are known from the experimental study that was carried out at NRC-IRC (Elmahdy et al. 2009), the exact airflow path is not. For modeling purposes, the possible air leakage paths through the wall assembly are defined based on experimental work observations and experience. Figure 5 and Figure 6 show the assumed air leakage path in the glass fibre and SPF insulated wall assemblies. In both walls the entry and exit points for the air are the same: a 3 mm gap between the sheathing boards (OSBs), and the interior electrical outlet, respectively. But the airflow paths between the entry and exit points are different in the two wall assemblies. In the case of the glass fibre insulated wall assembly, the air distributed throughout the insulation. Whereas in the case of SPF insulated wall, the air flows where there is wood-wood interface, more specifically, at the contact surface of the studs and sheathing boards as well as top/bottom plate and stud connections.

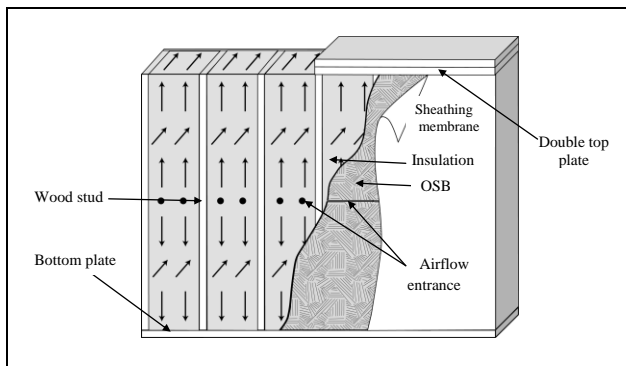


**Figure 5. Assumed airflow path in the glass fibre insulated wall assembly**

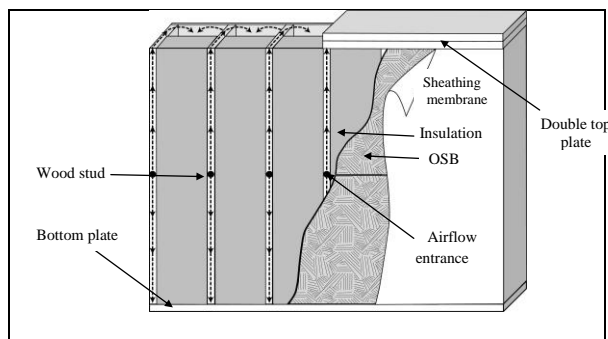


**Figure 6. Assumed airflow path in the SPF insulated wall assembly**

## General simulation assumptions

The combined conduction-convection simulations are carried out under the following assumptions:

- The layers of materials are in perfect contact, except for wood-wood interfaces.
- The condition at the perimeter of the wall assembly is adiabatic (no heat loss).
- The airflow path is predefined.
- The stud cavity is uniformly and completely filled with glass fibre insulation (in WER 1 and WER 5)
- The stud cavity is filled with 3" thick and uniform SPF (in WER 2, WER 3A, WER 3B and WER 4 walls).

## SIMULATION RESULTS

The simulations are carried out at steady outdoor and indoor temperatures of  $-20^{\circ}\text{C}$  and  $20^{\circ}\text{C}$ , respectively. A heat transfer coefficient of  $8 \text{ W}/(\text{K}\cdot\text{m}^2)$  is assumed for both interior and exterior surfaces. The RSI of the walls are calculated using the results of the steady state heat transfer conditions. In the numerical simulation, the steady state condition is assumed to be reached when the total heat fluxes at the weather and room sides, referred to in Figure 7 as left and right boundaries respectively, are equal. This condition is monitored during the simulation period. Figure 7 shows a typical monitoring situation where a wall assembly reached a steady state condition after two days in the five day simulation period.

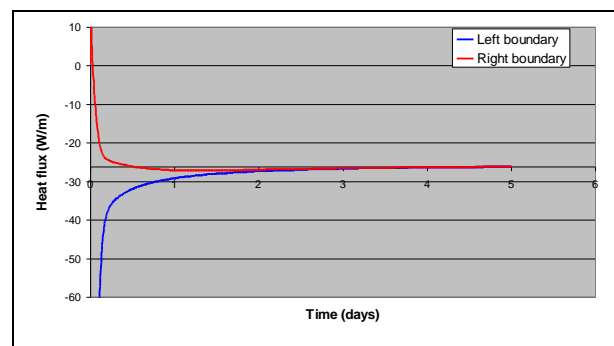


**Figure 7. Time histories of the transient heat fluxes at the wall boundaries. As steady state condition approaches, the heat fluxes through the boundaries converge.**

For the wall systems with 'window' (WER 3B, WER 4 and WER 5), Equations (7) and (8) are modified to Equations (9) and (10), respectively, to account for the heat transfer through the window and its frame. In the

experiment as well as this study, the window space is filled with a 4” thick extruded polystyrene (XPS) board. The heat flow through the ‘window’ and window frame are assumed to be one-dimensional. Thus, for given boundary conditions (indoor and outdoor temperatures), the total heat flow ( $Q_{wf}$ ) is calculated using the respective areas and thermal conductivity values given in Table 1.

$$RSI = A \frac{DT}{(q_v A_v + q_h A_h + q_j A_j + Q_{wf})} - R_s \quad (9)$$

$$RSI^* = A \frac{DT}{(q_v A_v + q_h A_h + q_j A_j + Q_{wf} + Q_{air})} - R_s \quad (10)$$

$$Q_{wf} = q_w A_w + q_f A_f$$

Where  $Q_{wf}$  is the total heat flow through the ‘window’ and window frame, and  $q_w$ ,  $A_w$ ,  $q_f$  and  $A_f$  are the heat fluxes and areas of the ‘window’ and window frame, respectively.

The effective RSI values of the wall systems for a temperature difference of 40°C and 0, 75 and 150 Pa pressure differences are calculated using Equation 7, 8, 9 or 10 (depending on the test scenario), and presented along with the corresponding GHB experimental results (cases with no air leakage, 0 Pa) in Table 3.

**Table 3. RSI values of the six walls as determined by computer model and experiment**

| Wall thermal resistance |                  |      |      |            |
|-------------------------|------------------|------|------|------------|
| RSI @ ΔT=40 K W(m².K)   |                  |      |      |            |
| WALL ID                 | Modeling Results |      |      | Experiment |
|                         | ΔP Pa            |      |      |            |
|                         | 0                | 75   | 150  | ΔP=0       |
| WER 1                   | 3.29             | 1.99 | 1.37 | 3.24       |
| WER 2                   | 3.58             | 3.40 | 3.30 | 3.60       |
| WER 3A                  | 3.42             | 3.05 | 2.94 | 3.67       |
| WER 3B                  | 2.91             | 2.73 | 2.60 | 3.00       |
| WER 4                   | 3.00             | 2.62 | 2.29 | 3.48       |
| WER 5                   | 2.75             | 1.24 | 0.82 | 2.78       |

The deviations between the simulation and experimental results are 1.5, 0.5, 6.8, 3, 13.8 and 1% for the WER 1, WER 2, WER 3A, WER 3B, WER 4 and WER 5. All of the deviations with the exception of WER 3A and WER 4, are under 6%, which is the uncertainty of the experimental measurement. The modeling assumption of ‘uniform SPF thickness’ might be the primary reason for the high deviations between

the modeling and experimental results in WER 3A and WER 4. Figure 8 shows a section of the WER 3A wall system that is tested in the GHB. As shown in the photo, the SPF thickness is not uniform, and the uniform thickness assumption in the modeling yields a result different from the experimental test result.



**Figure 8. Uneven SPF insulation thickness in WER 3A**

Figure 9 shows the apparent RSI at different pressure differences. Generally, the apparent RSI values of wall assemblies with glass fibre insulation decrease significantly at high pressure difference compared to that of the wall assemblies with SPF insulation. This is attributed to the low air leakage characteristics of the SPF wall system (see Table 2).

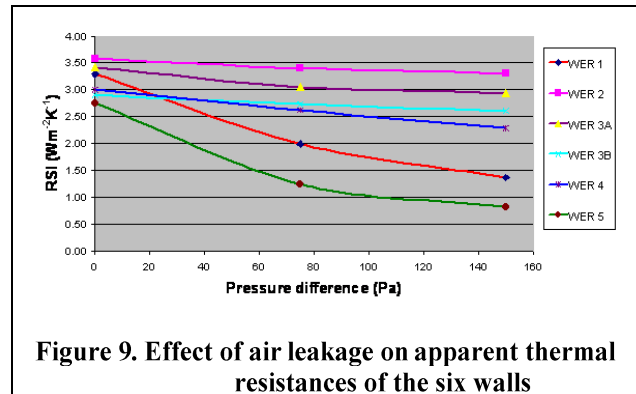


**Figure 9. Effect of air leakage on apparent thermal resistances of the six walls**

## CONCLUSIONS

The procedure outlined in this paper enables the analysis of the combined conduction-heat transfer of different wall systems.

--The methodology adopted in this paper helps to capture the three dimensional heat transfer in wall

systems with glass fibre and spray foam insulations by integrating two dimensional and one-dimensional thermal analysis.

--The modeling result agrees very well with the experimental data.

--The assumption of uniform insulation thickness in modeling is the main source of error (deviation from the experiment).

--For a given pressure difference, the air leakage in walls with glass fibre insulation and lapped polyethylene air barrier is significantly higher than that of walls with SPF.

--The apparent RSI values of wall assemblies with glass fibre insulation and lapped polyethylene air barrier decrease significantly compared to that of the wall assemblies with SPF insulation. This is attributed to the low air leakage characteristics of the SPF wall system

--High pressure difference significantly reduces the thermal resistance of the walls with glass fibre insulation and lapped polyethylene air barrier in comparison with the walls with SPF. Due to the airflow through gaps in the polyethylene and electrical outlet and then through the glass fibre insulation, the isotherm lines are distorted following the airflow path.

--Finally, it is important to have a good air barrier system to reduce air leakage, this is more important in walls with glass fibre insulation and lapped polyethylene air barrier, since the air short-circuits the thermal insulation capacity of the glass fibre.

## REFERENCES

- Bomberg, M.T.; Kumaran, M.K. 1989. "Report on sprayed polyurethane foam with alternative blowing agents," CFCs and the Polyurethane Industry: Vol 2: (A Compilation of Technical Publications) pp. 112-128, 1989, (NRCC-31113) (IRC-P-1638).
- Kumaran, M.K.; Bomberg, M.T. 1990 "Thermal performance of sprayed polyurethane foam insulation with alternative blowing agents," Journal of Thermal Insulation, 14, (July), pp. 43-57, July, 1990, (NRCC-32365) (IRC-P-1695).
- Elmahdy, A. H., Maref, W. Swinton, M. C., Tariku, F. 2009. Energy rating of polyurethane spray foamed walls: procedures and preliminary results. 4th International Building Physics Conference, Istanbul, Turkey, 15-18 June, 2009.
- Maref, W., H. Elmahdy, M. C. Swinton and F. Tariku. 2009 Assessment of Energy Rating of Polyurethane Spray Walls: Procedure and Interim Results, ASTM 2<sup>nd</sup> Symposium on Heat-Air-Moisture Transport: Measurements and Implications in Buildings, Sponsored by ASTM C16 on Thermal Insulation, April 19-20, 2009, Vancouver, British Columbia, Canada.
- Di Lenardo, Canadian Construction Materials Center (CCMC). Technical Guide for Air Barrier Systems for Exterior Walls of Low-Rise Buildings, Masterformat Section 07272, National Research Council of Canada, 1996.
- Karagiozis, A.N. 1993. Overview of the 2-D hygrothermal heat-moisture transport model LATENITE. Internal IRC/BPL Report, IRC/NRC, National Research Council of Canada.
- Karagiozis, A.N. 1997. Analysis of the hygrothermal behavior of residential high-rise building components. Client report A-3052, IRC/NRC, National Research Council of Canada.
- Salonvaara, M.H. and Karagiozis, A.N. 1994. Moisture transport in building envelopes using an approximate factorization solution method. Second Annual Conference of the CFD Society of Canada. Toronto, Canada, pp. 317-326.
- Hens, H. 1996. Heat, Air and Moisture Transport, Final Report, Vol. 1, Task 1: Modeling. International Energy Agency Annex 24, Laboratorium Bouwfysica, K. U.-Leuven, Belgium
- Maref, W., Lacasse, M. A, Kumaran, M.K. and Swinton, M.C. 2002a. Advanced Hygrothermal Model-HygIRC: Laboratory Measurements and Benchmarking, 12th International Heat Transfer Conference (18-23 August 2002, Grenoble, France)
- Maref, W., Lacasse, M. A, Kumaran, M.K. and Swinton, M.C. 2002b. Benchmarking of the Advanced Hygrothermal Model-HygIRC with Mid Scale Experiments, eSim Conference-IBPSA-Canada- Montreal (Sept. 12-13, 2002)
- Tariku, F.; Kumaran, M. K. 2006. Hygrothermal Modeling of Aerated Concrete Wall and Comparison With Field Experiment, Proceedings of the 3rd International Building Physics/Engineering Conference, August 26-31, Montreal, Canada, pp 321-328
- Maref, W. & Tariku, F., 2007. Assessment of Vapour Barrier Performance and Drying Effects Toward the Interior for Canadian Climate Report for CertainTeed Corporation, National Research Council Canada, Institute for Research in Construction, Canada, June 2007.
- Tariku, F.; Cornick, S.; Lacasse, M. 2007. Simulation of Wind-Driven Rain Effects on the Performance of a Stucco-Clad Wall, Proceedings of Thermal Performance of the Exterior Envelopes of Whole

Buildings X International Conference, Dec. 2-7,  
Clearwater, FL

Kumaran, K.; Lackey, J.; Normandin, N.; Tariku, F.;  
van Reenen, D. 2002. A Thermal and Moisture  
Transport Property Database for Common Building  
and Insulating Materials, Final Report—ASHRAE  
Research Project 1018-RP, 229 pgs.

Elmahdy, A.H., Maref, Tariku, F.; M., Swinton, M.,  
Glazer, R.; Nicholls, M.; Nunes, N. (2009).  
Development of Energy Rating of Field Installed  
Spray Polyurethane Foam Wall Assemblies.  
WER, Final Report-1, NRC Institute for  
Research in Construction, pp. 77